Int J Adv Manuf Technol (2017) 88:3319–3327
DOI 10.1007/s00170-016-8989-2

ORIGINAL ARTICLE

Chip control in the dry machining of hardened AISI 1045 steel

X. P. Zhang[1] · **S. B. Wu**[1]

Received: 8 October 2015 / Accepted: 30 May 2016 / Published online: 20 June 2016

Abstract Hard machining has been recognized as an effective and efficient manufacturing process to replace the grinding of hardened material. To achieve a successful implementation of hard machining, chip morphology regulation is crucial since serrated chip morphology is desirable for breakability, collection, and automation. This study aims to address the critical factors in controlling the micro- and macro-chip morphologies in the hard turning of hardened AISI 1045 steel by using PCBN tool with chip breaker grooves to cover a wide range of machining parameters. Microscopic and macroscopic chip morphologies were measured, analyzed, and correlated with machining parameters and chip breaker. Experimental results demonstrate that high-speed machining is a substantial prerequisite for generating serrated chips by generating adiabatic shear bands and fracture bands, higher feed rate, and uncut depth are assistants to promote serrated chip when machining speed reaches its critical number. The bending force resulted from breaker grooves helps serrated chips break into 1~3 cm lengths at macroscopic level. Periodic fluctuation of cutting forces along three directions was identified during the machining of hardened AISI 1045 steel at high machining speeds. This study suggests a feasible implementation of dry hard turning into industry applications.

Keywords Dry hard machining · Hardened AISI 1045 steel · Serrated chip morphology · Chip breaker

1 Introduction

Hard turning is performed on materials with hardness within the 45–68 Rockwell range using a variety of tipped or solid cutting inserts, preferably CBN [1]. Hard machining of hardened steel has been regarded as an effective and feasible substitution for grinding process to achieve a superior surface integrity [2]. However, successful hard turning application highlights several concerns related to machine tool, cutting tools [3, 4], machining parameters [5], coolant conditions [6, 7], chip morphology [8–11], cutting force [12], and surface integrity [13–17]. Among those factors, chip morphology regulation at both micro and macro level is significantly crucial consideration since serrated chips and the proper lengths are desirable for their breakability, collection, and automation in achieving successful industry implementation. Komanduri et al. [18] conducted experiments on AISI 4340 steel at various speeds with the highest speed up to 2500 m/min. Chips were found to be continuous at the range of 30 to 60 m/min. Fully developed catastrophic shear bands separated by large areas (segments) of relatively less deformed material were observed in the chips at cutting speeds above 275 m/min. Duan and Zhang [19] indicated that serrated chip formation was likely due to adiabatic shear instability that occurred in the primary shear zones. Gu et al. [20] proposed an adiabatic shear localized fracture (ASLF) theory to explain the final stage of adiabatic shear evolution. They presented that complete ASLF in isolated segmentation formation should be above the cutting speed of 1300 m/min. Ye et al. [21] performed orthogonal (2D) high-speed cutting experiments on AISI 1045 steel. The research reveals that there was transition of chip morphology from

Electronic supplementary material The online version of this article (doi:10.1007/s00170-016-8989-2) contains supplementary material, which is available to authorized users.

✉ X. P. Zhang
zhangxp@sjtu.edu.cn

S. B. Wu
sjtuwu@126.com

[1] School of Mechanical Engineering, Shanghai Jiao Tong University, Shanghai 200240, China

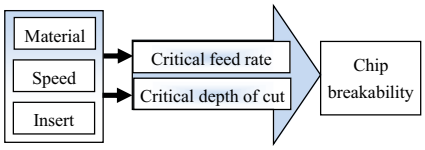

Fig. 1 Factors that influence chip breaking (Zhou [24])

continue to saw-tooth with increasing cutting speeds from 30 to 200 m/s. Those researches demonstrated that high-speed machining was a critical prerequisite for serrated chip morphology formation at micro level. However, serrated chip morphology only provides the prerequisite of final desirable chip lengths of chip at the macro level to facilitate industry automation. Generally, serrated chips are not completely separated, whereas the adiabatic shear bands in chip with low strength make it easier to break than original workpiece material. Generally, chip breaker is an important method to control chip morphology at the macro level by breaking chip into proper lengths with the help of bending force generated from the obstacle of cutting tool rake face [22, 23]. Zhou [24] concluded that chip breakability was determined by material property of workpiece, machining speed, insert geometry, and property, critical feed rate and depth of cut, as shown in Fig. 1. Many previous studies were done on the fundamentals of chip formation and breaking and attempts to develop chip-breaking criteria [25–35]. Chip curl is the key to understand chip space movement mechanism. Fang et al. [26] found that chip curl has three basic modes: up-curl, side-curl, and lateral curl. Jawahir et al. [32, 33] gave chip-up curl radius (R_0) equation to determine chip-breaking groove radius (R). This theory was used to optimize cutting tool design and control chip breaking [35].

The above analysis shows that tremendous studies have been performed on the mechanisms of serrated chip formation and chip breaking, however, few attentions have focused on the combination effect of serrated chip at micro level and chip breaker at the macro level. Besides, the roles of feed rate and cutting depth in developing serrated chip were not fully evaluated. This study aims to address the crucial factors in achieving desirable chips at micro and macro levels by experimental investigation into the machining of hardened AISI 1045 steel using PCBN tool with chip breaker covering a wide range of machining parameters. Microscopic and macroscopic chip morphologies were measured and correlated with machining parameters and chip breaker sequentially.

To achieve this objective, the research is arranged in this way: firstly, the effect of chip breaker on chip morphology and chip breaking is evaluated within the low machining speeds ranging from 110 to 276 m/min by varying feed rates and depths of cut; then the combination effect of high machining speed above 414 m/min and chip breaker on chip morphology and chip breaking is further determined. Finally, the feasibility of high-speed machining of hardened AISI 1045 steel in industry application is analyzed in terms of chip morphology, cutting force, and surface roughness.

2 Experiment procedure

2.1 Sample preparation

Sample workpiece was supplied as main spindle for machine tool. Detailed structure and geometrical dimension is shown in Fig. 2a. The hard turned region is the outer surfaces of the spindle with diameters of 80 and 88 mm, and a total length of 285 mm. The workpiece material was made of normalized

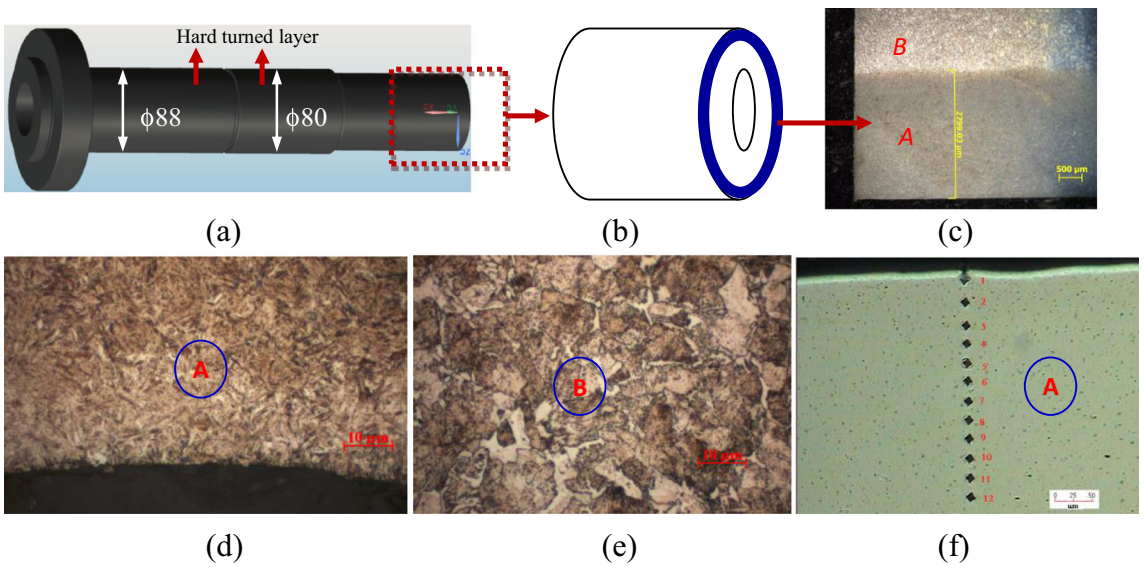

Fig. 2 Workpiece of normalized AISI steel with hardened layers: **a** main spindle; **b** hardened layer illustration; **c** hardened AISI steel layer with a depth of about 2.5 mm; **d** Optical image of hardened AISI 1045 steel referred as region "*A*"; **e** Optical image of the normalized AISI 1045 steel referred as region "*B*"; **f** Hardness measurement of hardened layer of AISI 1045 steel

Table 1 Chemical composition of hardened AISI 1045 steel

Chemical composition	C	Mn	P	S	Cr	Ni
Weighted (%)	0.42–0.50	0.50–0.18	0.04 (max)	0.05 (max)	0.25 (max)	0.25 (max)

AISI 1045 steel with a hardened layer in the surfaces of the main spindle, as shown in Fig. 2b, c.

Sample preparation procedure are as follows: (1) AISI 1045 steel bar was machined into main spindle for machine tool; (2) the main spindle was then quenched and tempered to a hardness of HRC45; and (3) surface layers were further hardened by means of medium frequency induction heating process to achieve the hardness of HRC52~58 within a penetration depth of about 2.5 mm. Thus the sample workpiece has two distinct microstructures, referred to as section "*A*" denoting a hardened AISI 1045 steel and section "*B*" denoting a normalized AISI 1045 steel, as shown in Fig. 2d–f. All machining experiments were performed on hardened layer under dry machining conditions. Chemical compositions of AISI 1045 steel are listed in Table 1.

2.2 Tool holder and cutting tool

Tool holder used in the experiments was model DTGNL2525M16 provided by Sandvik Co. Cutting tool inserts were CBN of TNMA160408SV-E (BT7600) with six cutting edges provided by Zhengzhou Berlt Co., Ltd. Chip breaker grooves in the rake face were specifically designed to promote macroscopical chip curling and breaking by providing extra bending force on chip. The cutting inserts have a negative rake angle of −6°, clearance angle of 6°, and a 0.8-mm nose radius. The cutting tool and tool holder are shown in Fig. 3.

2.3 Machine tool and testing system

The sample spindle was turned on a lathe SL50 of high stiffness. The cutting tool was mounted on the Kistler Multicomponent Dynamometer (9257B). The cutting forces measurement system includes a charge amplifier (Kistler 5001), a spectrum analyzer (HP 3567A) and a PC for data acquisition and analysis, and the forces along cutting direction, axial direction, and radial (thrust) direction are denoted as F_c, F_f, and F_t, respectively, as shown in Fig. 4.

2.4 Experimental design

Experimental machining parameters were selected to fully consider present industry application range, recommendation range suggested by tool manufacturer, and high-speed range based on hard turning mechanism under dry machining conditions. The length of machined distance along axial direction is 5~15 mm. The selected machining parameters are listed in Table 2. Hard turning experiments were performed in two steps to sequentially evaluate the effects of machining parameters and breaker grooves on chip micro- and macro- morphology.

Firstly, it adopted Table 3 to determine the effects of conventional machining parameters and the breaker grooves on chip macro-morphology. These parameters can also be used for Taguchi method analysis by selecting corresponding experimental data. Second step implemented the high-speed machining parameters listed in Table 4 to evaluate the effect of break grooves on serrated chips. Each experiment was repeated using a new fresh cutting edge to eliminate the negative effect of possible tool wear.

3 Results analysis and discussion

Macroscopical chip morphologies were measured using the Stereomicroscope (Stemi 2000) and True Color Confocal Microscope for Materials Microscopy (Axio CSM 700) provided by Carl Zeiss Shanghai Co., Ltd. Full experimental results are

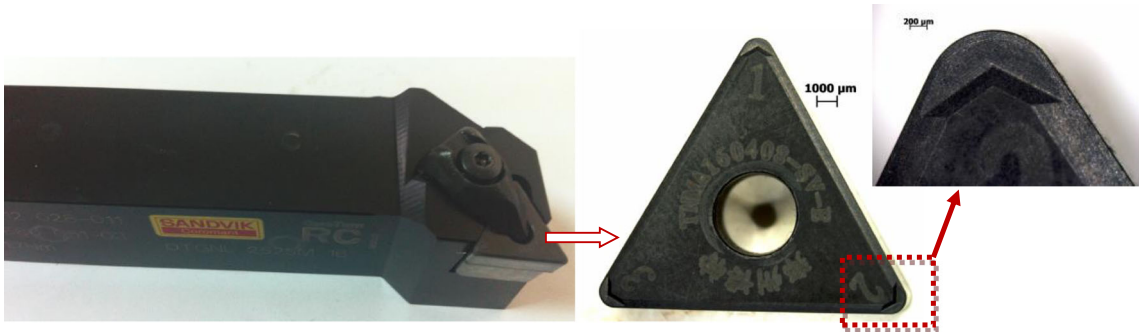

Fig. 3 PCBN cutting tool: **a** tool holder; **b** insert with chip breaker

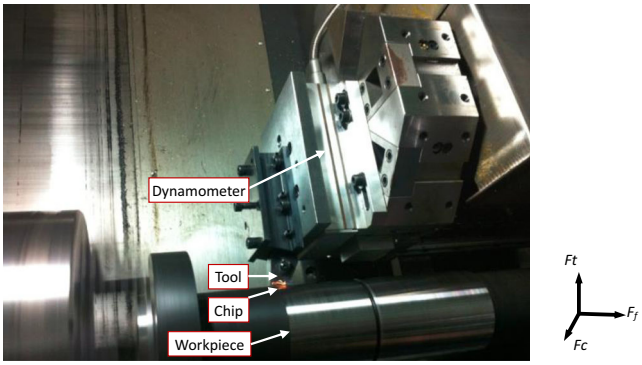

Fig. 4 Experimental setup of hard machining with cutting forces measurement system

shown in Supplementary Material 1, 2, and 3, which demonstrate experimental chip morphologies at magnifications of 20, 40, and 144 when uncut depths are 0.1, 0.2, and 0.3 mm, respectively.

Some results are shown in Figs. 5, 6, 7, 8, 9, and 10. These results demonstrate the effects of depth of cut, cutting speed, and feed rate on the transition from continuous chips to serrated chips. Continuous ribbon chips can be produced at low cutting speed of 110 m/min, and the chip thickness is relatively uniform. Fractures appear in the chips along the axial direction corresponding to axial force of F_f. It means that the chip is continuous along both the radial and cutting directions corresponding to thrust force (F_t) and cutting force (F_c). Smaller feed rate and breaker grooves facilitate chip macroscopical fluctuation along feed rate direction, as shown in Figs. 5 and 7. Chips demonstrate as saw-tooth morphology at higher cutting speed of 276 m/min. Deformation localizations and fractures can be observed along the three directions of axial, radial, and cutting corresponding to cutting forces of F_f, F_t, and F_c. However, no broken chips appeared even with the help of breaker grooves on tool rake face under the selections of feed rates and uncut depths.

Several related parameters can be selected to indicate the variation of chip morphology and the effects of machining parameters on chip morphology. For example, the macro fluctuation frequency along cutting forces f_c, can be used to calibrate the variation of chip morphology. The lower the feed rate, the higher the frequency of f_c, and the lower the depth of cut, the higher the frequency of f_c. Cutting speed has much less effect on the macro fluctuation frequency of f_c. Roughness on chip surface along cutting forces R_c can also be used to calibrate the variation of chip morphology. The higher the cutting speed, the value of roughness of R_c is higher.

Table 2 Experimental inputs of machining parameters

Machining parameters	Range
Cutting speeds (m/min)	110, 193, 276, 414, 552
Feed rates (mm/r)	0.05, 0.1, 0.15
Uncut depths (mm)	0.1, 0.2, 0.3

Table 3 Experiments with conventional machining parameters

Experiment no.	Cutting speeds v_c (m/min)	Feed rates f (mm/r)	Uncut depths a_p (mm)
1-1	110	0.05	0.1
1-2	110	0.1	0.1
1-3	110	0.15	0.1
1-4	193	0.05	0.1
1-5	193	0.1	0.1
1-6	193	0.15	0.1
1-7	276	0.05	0.1
1-8	276	0.1	0.1
1-9	276	0.15	0.1
2-1	110	0.05	0.2
2-2	110	0.1	0.2
2-3	110	0.15	0.2
2-4	193	0.05	0.2
2-5	193	0.1	0.2
2-6	193	0.15	0.2
2-7	276	0.05	0.2
2-8	276	0.1	0.2
2-9	276	0.15	0.2
3-1	110	0.05	0.3
3-2	110	0.1	0.3
3-3	110	0.15	0.3
3-4	193	0.05	0.3
3-5	193	0.1	0.3
3-6	193	0.15	0.3
3-7	276	0.05	0.3
3-8	276	0.1	0.3
3-9	276	0.15	0.3

4 Validation of the feasibility of high-speed hard turning

This section aims to address the combined effect of high-speed machining and chip breaker on chip morphology as well as cutting forces and surface roughness to support hard turning to substitute grinding of hardened AISI 1045 steel in industry application. Machining speeds were selected as 414 and 552 m/min, uncut chip as 0.3 and 0.2 mm, and feed rate as 0.15 mm/r. Experiments were performed and repeated three times using the same procedure described in section 2. Chips were collected and observed; cutting forces and surface roughness were measured to correlate with chip morphology in the high-speed machining of hardened AISI 1045 steel.

Table 4 Experiments with high-speed machining parameters

Experiment no.	Cutting speeds v_c (m/min)	Feed rates f (mm/r)	Uncut depths a_p (mm)
1	414	0.15	0.3
2	552	0.15	0.2

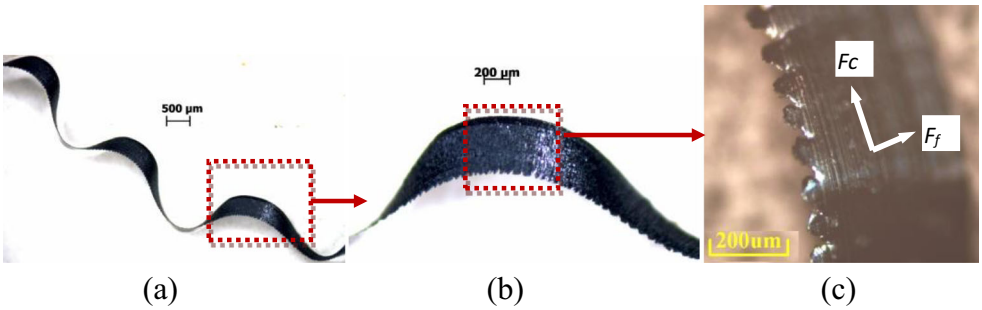

Fig. 5 Macroscopic chip morphologies at different magnifications ($a_p = 0.1$ mm, $v_c = 110$ m/min, $f = 0.05$ mm/r)

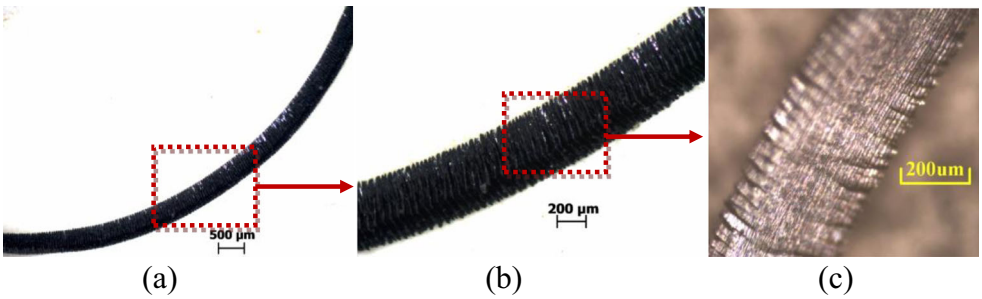

Fig. 6 Macroscopic chip morphologies at different magnifications ($a_p = 0.1$ mm, $v_c = 276$ m/min, $f = 0.15$ mm/r)

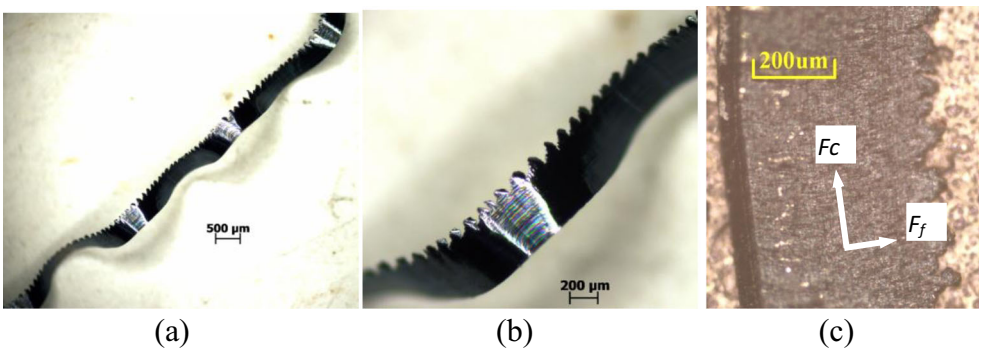

Fig. 7 Macroscopic chip morphologies at different magnifications ($a_p = 0.2$ mm, $v_c = 110$ m/min, $f = 0.05$ mm/r)

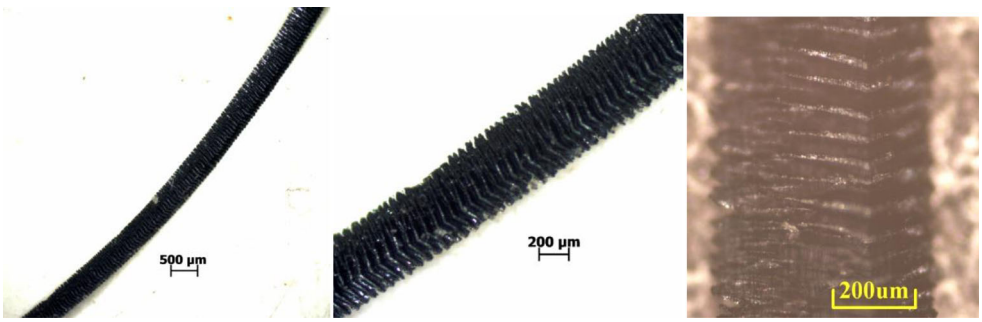

Fig. 8 Macroscopic chip morphologies at different magnifications ($a_p = 0.2$ mm, $v_c = 276$ m/min, $f = 0.15$ mm/r)

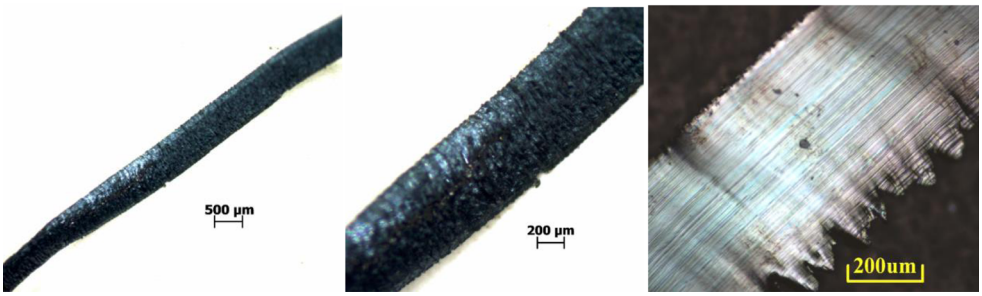

Fig. 9 Macroscopic chip morphologies at different magnifications ($a_p = 0.3$ mm, $v_c = 110$ m/min, $f = 0.05$ mm/r)

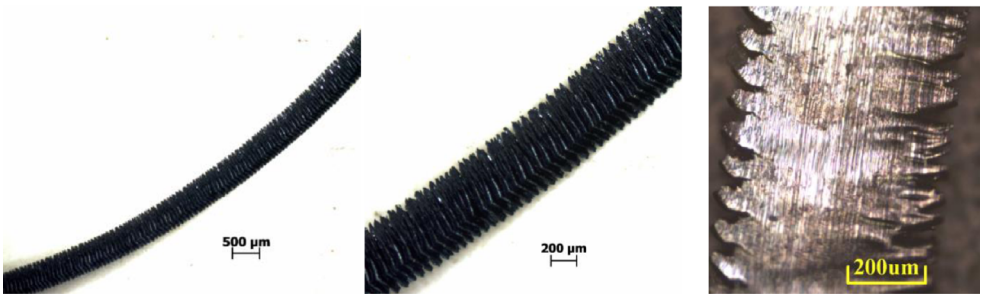

Fig. 10 Macroscopic chip morphologies at different magnifications ($a_p = 0.3$ mm, $v_c = 276$ m/min, $f = 0.15$ mm/r)

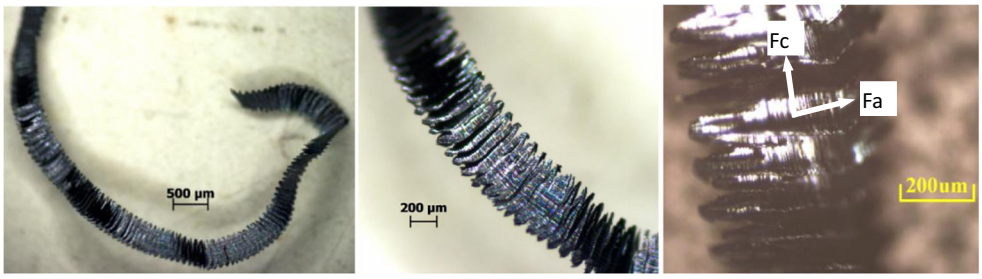

Fig. 11 Chip morphology at speed $v_c = 414$ m/min, feed rate $f = 0.15$ mm/r, and uncut depth $a_p = 0.3$ mm: **a** ×20; **b** ×50; **c** ×144

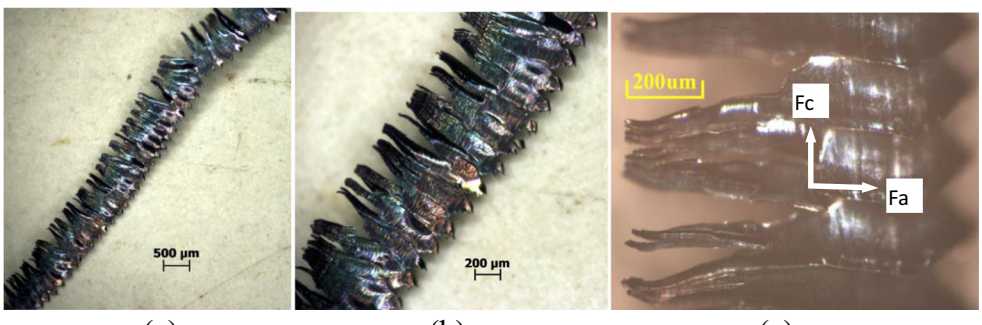

Fig. 12 Chip morphology at speed $v_c = 552$ m/min, feed rate $f = 0.15$ mm/r, and uncut depth $a_p = 0.2$ mm: **a** ×20; **b** ×50; **c** ×144

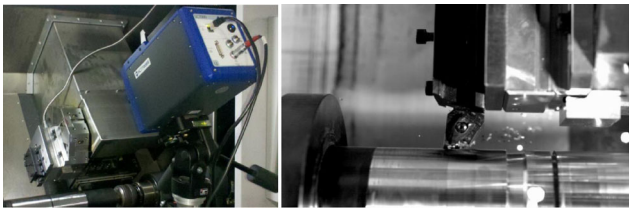

(a) (b)

Fig. 13 Recording of the high-speed hard turning of hardened AISI 1045 steel under dry conditions: **a** high-speed digital camera system; **b** Macroscopically broken serrated chips produced in hard turning

4.1 Chip morphology

Macroscopical chip morphologies are shown in Figs. 11 and 12. It clearly demonstrates that as cutting speed increases (414 and 552 m/min), serrated chipping took place in turning of hardened steel AISI 1045, and fractured shear bands can be observed regularly in the 3D primary shear zones along cutting direction, feed direction, and depth direction. The hard turning process was recorded by high-speed digital camera of Phantom v1210 aided with imagining software, as shown in Fig. 13. Repeated high-speed machining experiments proves that serrated chips were easily broken as short chips of 1~3 cm lengths with the help of breakers on the rake face of cutting tool by producing bending force on the chip. The experiments testify the feasibility to apply high-speed hard turning into actual finish machining application to achieve successful machining automations in terms of desirable macroscopical chips.

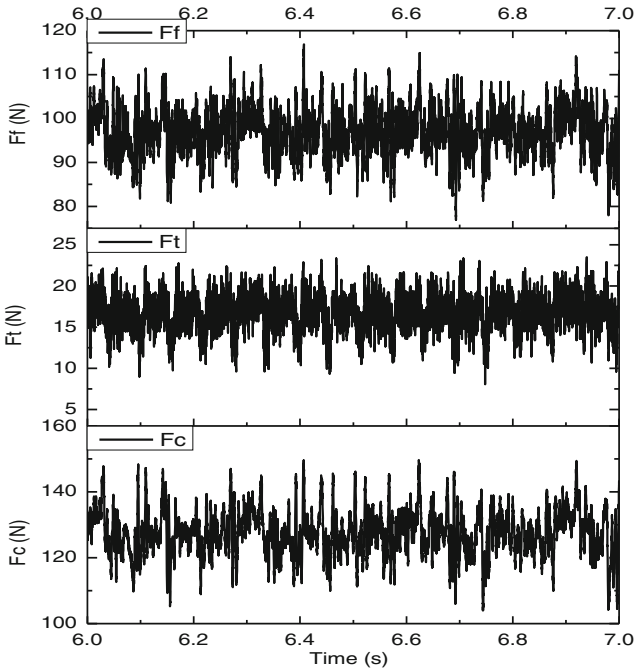

Fig. 15 Experimental cutting forces correspond to ribbon chips in the hard turning of hardened AISI 1045 steel at conventional speed of $v_c = 276$ m/min, feed rate $f = 0.1$ mm/r, and uncut depth $a_p = 0.2$ mm

4.2 Cutting forces

It was well known that machining forces were correlated with microscopic chip formation, macroscopic morphology development, curling, and breaking processes. This section demonstrates that cutting forces have cyclic characteristics in three directions as serrated chips were formed during the high-speed

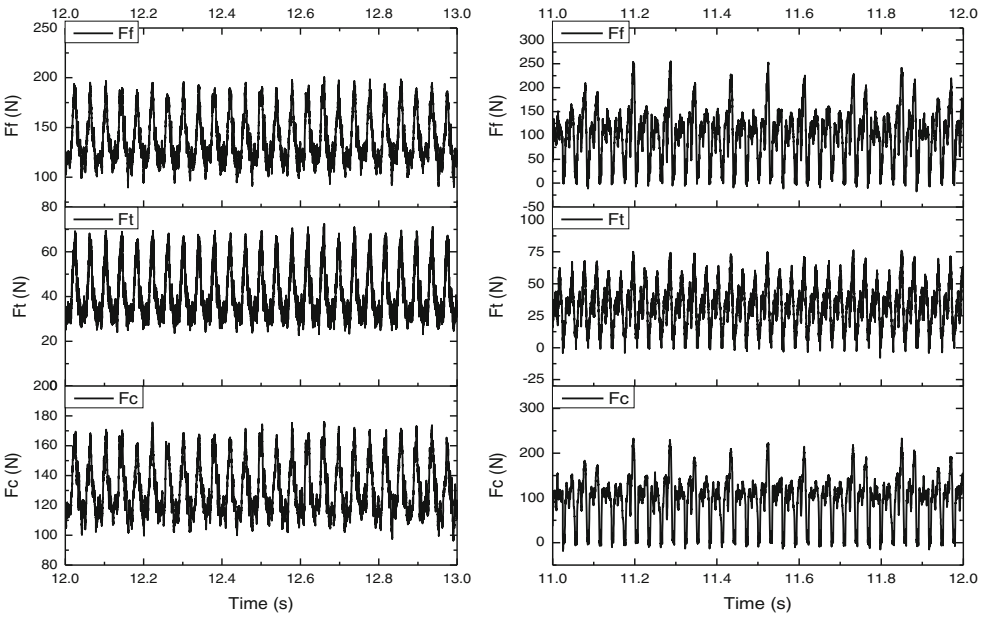

(a) (b)

Fig. 14 Experimental cutting forces correspond to serrated chips in the hard turning of hardened AISI 1045 steel at high speeds: **a** $v_c = 414$ m/min, $f = 0.15$ mm/r, $a_p = 0.3$ mm; **b** $v_c = 552$ m/min, $f = 0.15$ mm/r, $a_p = 0.2$ mm

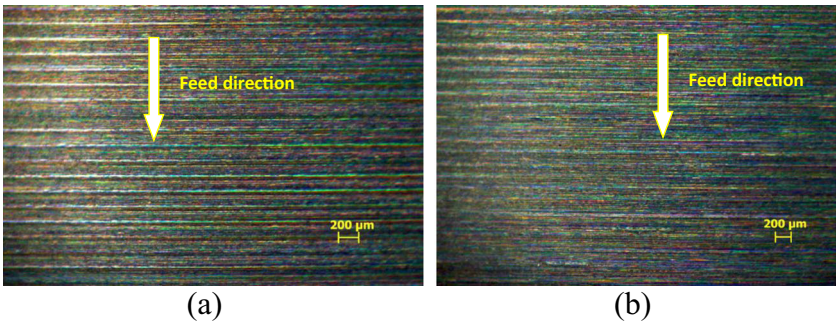

Fig. 16 Surface roughness measured by Stemi 2000: **a** cutting speed $v_c = 414$ m/min, feed rate $f = 0.15$ mm/r, and $a_p = 0.3$ mm; **b** cutting speed $v_c = 553$ m/min, feed rate $f = 0.15$ mm/r, and $a_p = 0.2$ mm

machining of hardened AISI 1045 steel, as shown in Fig. 14. The main frequencies are 25 and 33 Hz, respectively, corresponding to the cutting speeds of 414 and 552 m/min. These frequencies are the same as the rotation speeds of 1497 and 1997 rpm, respectively. Therefore, the periodicity in the cutting forces is due to workpiece rotation. However, the frequency of serrated chips formation is much higher. Although the main frequencies of cutting force are different from the frequencies of serrated chips, it is evident that cutting forces demonstrate periodic characteristics corresponding to serrated chips. Conversely, the measured cutting forces associated ribbon chips have no regular cyclic characteristics with ribbon chip morphology and local fracture behavior during hard turning process at conventional speeds, as presented in Fig. 15.

4.3 Surface roughness

Surface roughness is a crucial consideration to replace grinding as hard turning in finish machining of hardened materials. Surface roughness of the high-speed machined surface was measured using a Mitutoyo (China) SJ-210 portable device within the sampling length of 5 mm. Given feed rate of 0.15 mm/r, surface roughness ranges from 0.63 to 1.60 μm in the hard turning of hardened steel AISI 1045 at speeds of $v_c = 414$~552 m/min. According to previous research [17], surface roughness is the most sensitive to feed rate. Smaller feed rates produce superior surface finish. It means that surface finish generated from high-speed hard turning is capable of meeting the requirement of finish machining with selected smaller feed rates. Hard turning is feasible to be implemented in industry application since it can reach the same level as that achieved by grinding process in terms of surface roughness [36]. The scanning electron microscope (SEM) of hard turned surface roughness was also measured by Stereomicroscope Stemi 2000, as shown in Fig. 16.

5 Conclusion

This paper presents an investigation into the effects of machining parameters and chip breaker on chip micro- and macro-morphologies evolution in the hard turning of hardened AISI 1045 steel under dry conditions. An experimentally systematic analysis shows that low cutting speeds lead to continuous chip morphology regardless of feed rates and uncut depths within the range of selected machining parameters. In this case, chip breaker has limited capability to break the continuous chip into desirable lengths without effective fractured shear bands in chip. High machining speeds result in serrated chips with fractured shear bands. This type of serrated chipping can be easily broken into 1~3 cm length macroscopic chips with the help of bending force generated from chip breakers. Periodic fluctuation of cutting forces was identified to correspond to serrated chip morphology in hard turning of hardened AISI 1045 steel. With proper selection of feed rates and cutting depths, high-speed machining of hardened steel can produce desirable surface roughness. This study suggests a feasible implementation of dry hard turning into industry applications by producing macroscopically broken chips favorable for collection and machining automation.

Acknowledgments This research was supported by the National Science and Technology Major Project of the Ministry of Science and Technology of China (No. 2013ZX04012-052), and the National Natural Science Foundation of China (No. 51175331).

References

1. Bartarya G, Choudhury SK (2012) State of the art in hard turning. Int J Mach Tools Manuf 53:1–14
2. Liu CR, Mittal S (1996) Single-step superfinish hard machining: feasibility and feasible cutting conditions. Robot Comput Integr Manuf 12:15–27
3. Chinchanikar S, Choudhury SK (2013) Effect of work material hardness and cutting parameters on performance of coated carbide tool when turning hardened steel: an optimization approach. Measurement 46:1572–1584
4. Rogante M (2009) Wear characterization and tool performance of sintered carbide inserts during automatic machining of AISI 1045 steel. J Mater Process Technol 209:4776–4783
5. Chou YK, Evans CJ, Barash MM (2002) Experimental investigation on CBN turning of hardened AISI 52100 steel. J Mater Process Technol 124:274–283

6. Kramar D, Krajnik P, Kopac J (2010) Capability of high pressure cooling in the turning of surface hardened piston rods. J Mater Process Technol 210:212–218
7. Chinchanikar S, Choudhury SK (2015) Machining of hardened steel-experimental investigations, performance modeling and cooling techniques: a review. Int J Mach Tools Manuf 89:95–109
8. Shi J, Liu CR (2006) On predicting chip morphology and phase transformation in hard machining. Int J Adv Manuf Technol 27: 645–654
9. Simoneau A, Ng E, Elbestawi MA (2006) Chip formation during microscale cutting of a medium carbon steel. Int J Mach Tools Manuf 46:467–481
10. Rhim SH, Oh SI (2006) Prediction of serrated chip formation in metal cutting process with new flow stress model for AISI 1045 steel. J Mater Process Technol 171:417–422
11. Kharkevich AG, Venuvinod PK (2002) Extension of basic geometric analysis of 3-D chip forms in metal cutting to chips with obstacle-induced deformation. Int J Mach Tools Manuf 42:201–213
12. Matsumoto Y, Barash MM, Liu CR (1987) Cutting mechanism during machining of hardened steel. Mater Sci Technol 3:299–305
13. Shi J, Liu CR (2005) On predicting material softening effect in hard turning—part I: construction of material softening model. J Manuf Sci Eng 127:476–483
14. Shi J, Liu CR (2005) On predicting material softening effect in hard turning—part II finite element modeling and verification. J Manuf Sci Eng 127:484–491
15. Muñoz-Escalona P, Cassier Z (1998) Influence of the critical cutting speed on the surface finish of turned steel. Wear 218:103–109
16. Han S, Melkote SN, Haluska MS, Watkins TR (2008) White layer formation due to phase transformation in orthogonal machining of AISI 1045 annealed steel. Mater Sci Eng A 488:195–204
17. Zhang XP, Liu CR, Yao ZQ (2007) Experimental study and evaluation methodology on hard surface integrity. Int J Adv Manuf Technol 34:141–148
18. Komanduri R, Schroeder T, Hazra J, Turkovich BFV, Flom DG (1982) On the catastrophic shear instability in high-speed machining of an AISI 4340 steel. J Eng Ind 104:121–131
19. Duan CZ, Zhang LC (2012) Adiabatic shear banding in AISI 1045 steel during high speed machining: mechanisms of microstructural evolution. Mater Sci Eng A 532:111–119
20. Gu LY, Wang MJ, Duan CZ (2013) On adiabatic shear localized fracture during serrated chip evolution in high speed machining of hardened AISI 1045 steel. Int J Mech Sci 75:288–298
21. Ye GG, Xue SF, Ma W, Jiang MQ, Ling Z, Tong XH, Dai LH (2012) Cutting AISI 1045 steel at very high speeds. Int J Mach Tools Manuf 56:1–9
22. Lee YM, Yang SH, Chang SI (2006) Assessment of chip-breaking characteristics using new chip-breaking index. J Mater Process Technol 173:166–171
23. Kharkevich A, Venuvinod PK (1999) Basic geometric analysis of 3-D chip forms in metal cutting. Part 1: determining up-curl and side-curl radii. Int J Mach Tools Manuf 39:751–769
24. Zhou L (2001) Machining chip-breaking prediction with grooved inserts in steel turning, Ph.D. Research dissertation
25. Fang XD, Jawahir IS (1996) An analytical model for cyclic chip formation in 2-D machining with chip breaking. Ann CIRP 45:53–58
26. Fang N, Jawahir IS, Oxley PLB (2001) A universal slip-line model with non-unique solutions for machining with curled chip formation and a restricted contact tool. Int J Mech Sci 43:557–580
27. Fang N (1998) An improved model for oblique cutting and its application to chip-control research. J Mater Process Technol 79:79–85
28. Shinozuka J, Obikawa T, Shirakashi T (1996) Chip breaking analysis from the viewpoint of the optimum cutting tool geometry design. J Mater Process Technol 62:345–351
29. Kluft W, Konig W, Luttervelt CAV, Nakayama K, Pekelharing AJ (1979) Present knowledge of chip control. Ann CIRP, Keynote Paper 28:441–455
30. Nakayama K, Arai M, Kondo T (1981) Cutting tools with curved rake face—a means for breaking thin chips. Ann CIRP 30:5–8
31. Jiang CY, Zhang YZ, Chi ZJ (1984) Experimental research of the chip flow direction and its application to the chip control. Ann CIRP 33:81–84
32. Jawahir IS, Fang XD (1995) A knowledge-based approach for designing effective grooved chip breakers-2D and 3D chip flow, chip curl and chip breaking. Int J Adv Manuf Technol 10:225–239
33. Jawahir IS (1990) On the controllability of chip breaking cycles and modes of chip breaking in metal machining. Ann CIRP 39:47–51
34. Das NS, Chawla BS, Biswas CK (2005) An analysis of strain in chip breaking using slip-line field theory with adhesion friction at chip/tool interface. J Mater Process Technol 170:509–515
35. Kim HG, Sim JH, Kweon HJ (2009) Performance evaluation of chip breaker utilizing neural network. J Mater Process Technol 209:647–656
36. Liu CR, Mittal S (1995) Single-step superfinish hard machining: feasibility and feasible cutting condition. Robot Comput Int Manuf 12:15–27